OPTICA

Helico-conical vector beams for intensity and polarization 3D light shaping

Andrea Vogliardi,[1,2] Daniele Bonaldo,[2,3] Simone Dal Zilio,[4] Filippo Romanato,[1,2,4] and Gianluca Ruffato[1,2,3,*]

[1]Department of Physics and Astronomy 'G. Galilei', University of Padova, via Marzolo 8, 35131, Padova, Italy
[2]Padua Quantum Technologies Research Center, University of Padova, via Gradenigo 6, 35131, Padova, Italy
[3]Department of Information Engineering, University of Padova, via Gradenigo 6, 35131, Padova, Italy
[4]CNR-IOM Istituto Officina dei Materiali, S.S. 14-Km. 163, 5–34149, Trieste, Italy
*gianluca.ruffato@unipd.it

Received 8 July 2024; revised 10 October 2024; accepted 21 October 2024; published 3 December 2024

While vector beams offer an intriguing way to structure optical beams and enhance light-based technologies across many fields, their generation remains a challenging task in practical applications. Disclosing an unprecedented manipulation of light at the subwavelength scale, metaoptics have inspired smart and efficient solutions for spatially variant polarization structuring. Concurrently, the generalization of non-separability in polarization and phase manipulation extends the vectorial nature beyond standard vector vortices. In this work, we present the design and test of dual-functional metasurfaces for the compact generation of a new type of vector beam, so-called helico-conical vector beam, providing an inhomogeneous polarization pattern over customizable one-arm or two-arm 3D spirals of light. These devices pave the way to integrated optical architectures for dynamic optical manipulation and trapping in many fields, from optofluidics to quantum computing.

https://doi.org/10.1364/OPTICA.535090

The ability to control, combine, and structure the properties of light beams has driven significant progress and inspired practical implementations across various domains, ranging from life sciences [1,2] to information and communication technology [3–5]. While polarization was initially ignored or treated as a free degree of freedom, vector beams [6] introduced the concept of non-separability between spin and angular momentum (OAM) states to realize spatially variant configurations of the electric field direction, further extending the possibilities and applications of structured light. As a matter of fact, the non-trivial combination of OAM and spin defines four-dimension subspaces with outstanding properties and applications in microscopy [7], optical lithography [8,9], communication, and encryption [10,11]. The vectorial nature can be revealed by placing a polarizer since the local component orthogonal to the polarization axis is filtered out at any point of the beam. The spatial dependence of polarization is then lost and converted into an intensity pattern of bright lobes, whose size, number, and position depend on the OAM carried by the constituent circularly polarized beams and on their relative phase. This suggests a simple method for vector beam analysis [12] and a smart solution to obtain a polarization-tunable constellation of intensity spots. The vectorial nature can be extended beyond standard OAM modes, allowing, in principle, the realization of custom spatially variant polarization patterns over any desired optical beam. In particular, we consider here helico-conical beams (HCBs), which have recently attracted increasing attention as a special class of orbital angular momentum beams with peculiar spiral-like intensity profiles and self-healing properties [13–15].

It can be intriguing to merge these two paradigms to extend the capabilities of HCBs by including new degrees of freedom. To this aim, preliminary theoretical and experimental attempts were made [16] but the extension to the 4D subspaces has not been reached yet. Moreover, the generation of helico-conical beams usually exploits cumbersome optical setups housing many optical elements, such as spiral phase plates [17–19] or spatial light modulators [20] in complex interferential schemes. To this aim, the metasurface paradigm [21] can give miniaturization a step further, enabling the control of light in ways not previously possible [22,23].

In this paper, we present for the first time the compact generation of new 3D helico-conical beams having vectorial nature, proving the validity of an analytical description of their 3D intensity profiles and offering a paradigm for the design of custom polarization-tunable spot constellations. The key element is represented by dual-functional metasurfaces [24] guaranteeing the spin-decoupled manipulation of the input beam which is necessary to control and shape the two circular polarizations in parallel. Thus, it is possible to generate helico-conical vector beams (HCVBs) with non-separable spin and OAM combinations without the need for bulky setups.

As introduced by Alonzo in 2005 [13], helico-conical beams are generated by the product of helical and conical phase patterns, which is well described by the spiral axicon lens phase [18]:

$$\Gamma(r,\vartheta) = \exp\left\{-ia\left(\frac{r-r_0}{R}\right)(m\vartheta+\vartheta_0)\right\}, \qquad (1)$$

where r_0 and ϑ_0 are radial and azimuthal shifts, respectively; R is the radius of the optics; m represents the coefficient of the linear azimuthal gradient; and a is a dimensionless parameter. By

illuminating the phase pattern of Eq. (1) with a Gaussian beam, an HCB is generated carrying OAM with topological charge of the beam (TC) equal to $l_{\mathrm{SPIRAL}} = -am/R$ [16]. In such beams, due to the relationship between the conical and the helical phases, the amount of TC carried by the beam contributes to different amplitude light shaping. Recalling that vector beams are generated by a non-separable combination of opposite spin and OAM values, their peculiar polarization pattern along the ring relies on the independence of the intensity profile on the OAM sign [6,25]. To give the HCB a spatially variant polarization pattern along the spiral we need to define two new phase functions for the two circular polarization states, that is,

$$\phi^{\pm}(r,\vartheta) = \exp\left\{-ia\left(\frac{r-r_0}{R}\right)(m\vartheta+\vartheta_0) \pm n\vartheta - \frac{kr^2}{2f}\right\}, \tag{2}$$

including a new term, i.e., $n\vartheta$, which imparts a conical-independent phase gradient and has different signs for the two polarizations. The spin-independent focusing term $-kr^2/2f$ (where $k = 2\pi/\lambda$ is the wavenumber and f is the focal length) confines the 3D spiral shaping at the desired distance from the optical element [13]. With this new phase profile, the spin-dependent generated beam carries two TCs: $l_{\mathrm{SPIRAL}} = -am/R$, affecting the shape of the spiral, and $l_{VB} = \pm n$, which is responsible for the rotating polarization pattern along the intensity profile [25]. Moreover, it is possible to extend the phase function further by considering the generation of multiple twisting spirals using the phase equalization paradigm [26]:

$$\Phi^{\pm}(r,\vartheta) = \mathrm{angle}\left\{\sum_{i=1}^{T} A_i \cdot \phi^{\pm}{}_{r_{0,i},\vartheta_{0,i},a_i,m_i,n_i}(r,\vartheta)\right\}, \tag{3}$$

where T is the number of distinct spiral arms, and $\{A_i\}$ are complex parameters controlling the relative amplitude and phase of each spiral arm. In our case of interest, considering the T-fold rotational symmetry of the output pattern, the complex weights are set equal to 1. To implement the vector beams paradigm compactly, we exploited the dual functional mechanism. The metaoptics are designed as a squared digital lattice of anisotropic nanoantennas, known as meta-atoms, working in the subwavelength regime and acting as half-wave plates (HWPs). Each meta-atom can be modeled with a Jones matrix J having a spin-decoupled behavior on right-handed ($|R\rangle$) and left-handed ($|L\rangle$) circular polarization states, as it follows [24]:

$$J|L\rangle = -i\Omega_{\mathrm{Dyn}}\Omega^{+}_{\mathrm{Geo}}|R\rangle = e^{i\Phi^{+}}|R\rangle, \tag{4}$$

$$J|R\rangle = -i\Omega_{\mathrm{Dyn}}\Omega^{-}_{\mathrm{Geo}}|L\rangle = e^{i\Phi^{-}}|L\rangle, \tag{5}$$

where $\Omega_{\mathrm{Dyn}} = e^{i(\delta_x+\delta_y)/2}$ is the dynamic phase contribution, δ_y and δ_x are the phase delays experienced by linear polarizations parallel to the ordinary and extraordinary axes of the metaatom, and $\Omega^{\pm}_{\mathrm{Geo}} = e^{\pm 2i\varphi}$ is the spin-decoupled contribution given by the geometric phase imparted by a φ-rotation of the metaunit on the plane. Inverting the above relations, it is easy to extract the values of dynamic and geometric phases required to impart the desired patterns $\Phi^{\pm}$ at any point of the metasurface ensuring respect for the HWP conditions $\delta_y = \delta_x + \pi$, and $\lfloor T_x \rfloor = \lfloor T_y \rfloor$ [24].

As a consequence of the linearity of the metaoptics, the non-separable combinations of spin and OAM are obtained under illumination with linearly polarized states $|\theta\rangle = [\cos\theta \ \sin\theta]^T$:

$$J|\theta\rangle = \Lambda^{+}e^{i\Phi^{-}}|L\rangle + \Lambda^{-}e^{i\Phi^{+}}|R\rangle, \tag{6}$$

where $\Lambda^{\pm} = e^{\pm i\theta}$ is the phase contribution due to the input polarization angle. After propagation, the fields in Eq. (6) form HCVBs on the focal plane of the optical element under illumination with a Gaussian beam. Moreover, it is possible to move to the anti-vortex state by inverting the signs in the $\Phi_{\pm l}$ terms or inserting a zero-order HWP in cascade to the same metaoptics. Finally, to design the 3D shape generated beam, we considered the caustic behavior of the HCBs. Applying the stationary phase approximation [27], we can obtain the parametric curves describing the intensity profile at a distance z:

$$u = \frac{z}{k}\left[-\frac{am}{R}(\vartheta\cos\vartheta - \sin\vartheta)\right] + \rho\cos\vartheta\left(1-\frac{z}{f}\right) - \frac{z}{k}\frac{n\sin\vartheta}{\rho}, \tag{7}$$

$$v = \frac{z}{k}\left[-\frac{am}{R}(\vartheta\sin\vartheta + \cos\vartheta)\right] + \rho\sin\vartheta\left(1-\frac{z}{f}\right) + \frac{z}{k}\frac{n\cos\vartheta}{\rho}, \tag{8}$$

where (u, v) are Cartesian coordinates on the plane; $\vartheta = \arctan(y/x)$; ρ is a scaling parameter equal to half the input waist w_0; and a, R, m, n, f are parameters of helico-conical beams as defined in Eq. (2), with $r_0 = \vartheta_0 = 0$.

Using FEM simulations (COMSOL Multiphysics) we identified a set of 13 different silicon meta-atoms of 850 nm height having an equispaced discretization of the dynamic phases and satisfying the HWP conditions at 1310 nm. This library guarantees the subwavelength regime and provides an average transmission of 75% over the whole metasurface [24,25]. Applying the abovementioned approach, we designed three different circular metaoptics with a diameter of 600 μm. The first one encodes a single-arm HCVB ($T = 1$) having a spiral TC equal to 10 ($a = -10$, $m = 1$) in an anti-vortex state of order 5 ($n = -5$ so $\ell_{\mathrm{VB}} = \pm n = \mp 5$). The second metasurface generates a two-arm HCVB ($T = 2$, $A_1 = A_2 = 1$) with opposite spiral TC ($a_1 = -10$, $a_2 = +10$, $m_1 = m_2 = 1$) in the same vortex state of order 3. Finally, the third sample generates a two-arm HCVB ($T = 2$) with opposite spiral TC ($a_1 = -10$, $a_2 = +10$, and $m_1 = m_2 = 1$) in opposite vectorial states of order 3, i.e., anti-vortex ($n_1 = -3$) and vortex ($n_2 = +3$), respectively. All the samples encoded a focusing term with $f = 1.5$ mm. Details of the phase patterns are reported in Fig. 1.

A custom MATLAB code was employed to simulate the theoretical optical response. The simulation exploited the Fresnel propagator within a squared window having the same size as the metaoptics (i.e., 600 μm), pixel size of 600 nm, and illumination by a Gaussian beam with a waist (w_0) of 150 μm. As depicted in Fig. 1, we obtain the peculiar polarization patterns by illuminating with a linearly polarized light [i.e., horizontal, $\theta = \pi/2$ in Eq. (6)]. In particular, $|2n|$ polarization rotations can be noticed, leading to a $|2n|$ multi-spot intensity pattern after filtering the beam with a linear polarizer as analyzer (rotated by an angle $\Psi = 0$ with respect to the x-axis).

Metaoptics fabrication underwent a two-step process: high-resolution electron beam lithography (EBL) of a thin resist layer spun over a Si wafer, followed by inductively coupled plasma–reactive ion etching (ICP-RIE) for pattern transfer to the substrate. The procedure is described in detail in [24] (Fig. 2).

The optical behavior was characterized using the fiber output of a DFB laser ($\lambda = 1310$ nm, 1310LD34 1-2-2-1 CCSI, AeroDiode) collimated, linearly polarized, and resized using

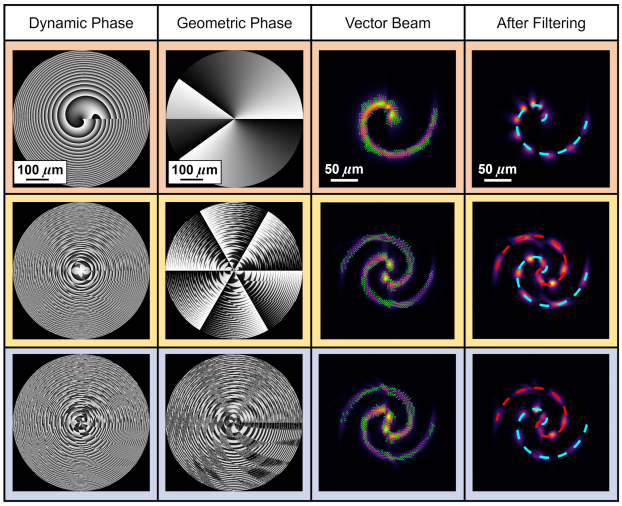

Fig. 1. The first two columns show the encoded dynamic and geometric phases, respectively, of the three designed metasurfaces. Grayscale intensity ranges from 0 (black) to 2π. The third column depicts the simulations of the generated vector beams with their polarization pattern under illumination with a horizontally polarized Gaussian beam. The last column shows the simulated intensity pattern after filtering the vector beam with a linear polarizer. The dashed lines refer to the model in Eqs. (7) and (8).

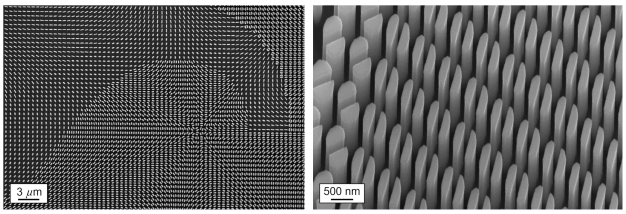

Fig. 2. Top-view SEM inspections of a fabricated silicon metasurface at different magnifications. It is worth noting the constituent different metaunits, equispaced and rotated by different angles.

a $4f$ system and a reflective SLM (X13267-08, Hamamatsu, pixel 12.5 μm) to produce a Gaussian beam of the desired waist (i.e., 150 μm). Finally, a 20x objective (20X Plan Apochromat Objective, 480–1800 nm, 0.40 NA, 20.0 mm WD, Mitutoyo) conjugated to a NIR camera (WiDy SWIR 640U-S, pixel 12.5 μm) collected the structured beam. In Fig. 3, we report the acquisition of the generated HCVBs at the design focal length $f = 1.5$ mm. The samples were illuminated with horizontal polarization, and the output vectorial beam was analyzed with a rotating linear polarizer. The experimental transmission is around 70%. In all three cases, the generation of vector beams was confirmed by the formation in each spiral arm of a number of bright spots equal to twice the conical-independent TC.

Considering the first metasurface, a single HCVB in the antivortex state was generated, as confirmed by a clockwise rotation of the sequence of spots (Fig. 3) under a counterclockwise rotation of the analyzer. In the second row of Fig. 3, the optical response of the second metaoptics is reported. In this case, two spiral arms are generated having opposite conical-dependent TC (same shape but specular direction), and the same conical-independent TC as for both arms the petal-like patterns rotate in the same direction of the rotating analyzer. In the last row, referring to the third metasurface,

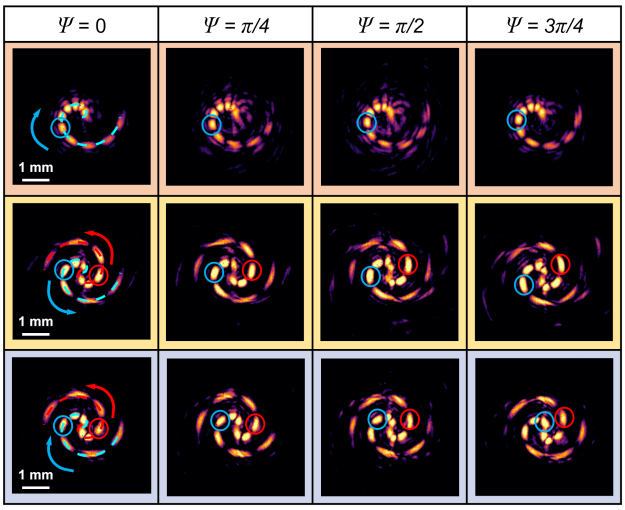

Fig. 3. Experimental characterization of the generated vector beams at the focal plane after filtering with a linear polarizer rotated by different angles. For each vector beam, $2|n|$ petal-like spots appear along each spiral arm, their rotation direction depending on the vectorial state. The dashed lines refer to the model in Eqs. (7) and (8).

the analysis confirms the generation of two arms with both opposite conical-dependent and opposite conical-independent TCs as matched by opposite rotation of the intensity multi-spot patterns.

Finally, we evaluated the 3D vectorial shaping acquiring the optical responses in the nearby of the design focal plane

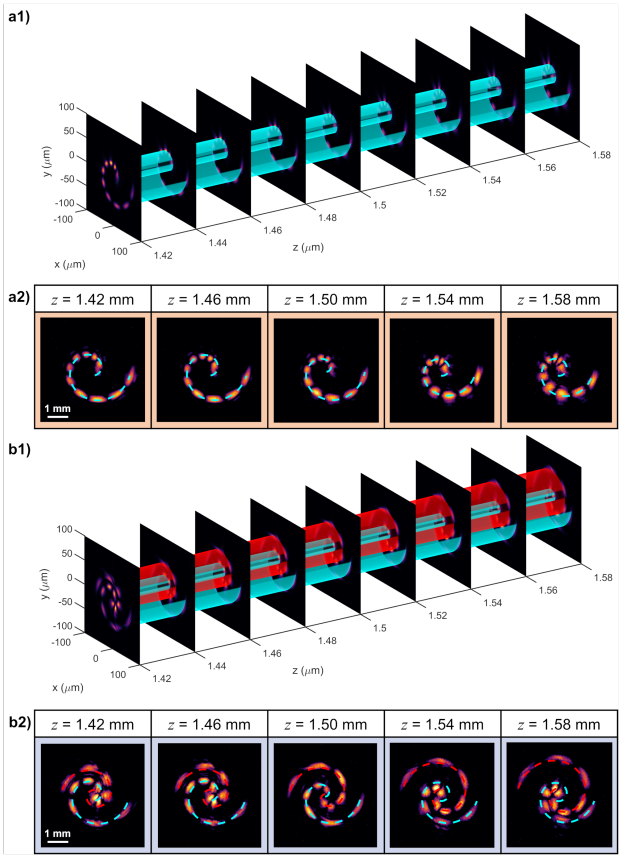

Fig. 4. Simulated (a1), (b1) and experimental (a2), (b2) analyses of the 3D polarization optical response of the metaoptics depicted in the first and second rows of Fig. 1. The HCVBs follow the caustic-like 3D path described by Eqs. (7) and (8), while preserving the vectorial state.

($z = f \pm 80$ μm). We started evaluating the theoretical 3D intensity shaping by implementing Eqs. (7) and (8), related to the caustic evolution of HCBs, with the design parameters. Then, we compared the theoretical shaping with the experimental one. As shown in Fig. 4, the experimental results of the first metasurface agree perfectly with the theoretical simulations with a shrinking of the vectorial spiral in the range of propagation from 1.42 mm to 1.58 mm (see Visualization 1, Visualization 2, Visualization 3, Visualization 4, Visualization 5, Visualization 6). Moreover, the same overlapping is obtained for the second metasurface, where the two-arm HCVBs exhibit complementary shrinking and expansion due to the opposite conical-dependent TC. It is worth noting that the same result can be obtained with the third metasurface as the "shaping" is related to the conical-dependent parameters and not to the non-dependent terms.

In conclusion, we have demonstrated, for the first time, the compact generation of helico-conical vector beams using a single dual-functional metasurface. By combining the control of dynamic and geometric phases, our approach enables parallel processing of both circular polarizations to impart beam reshaping with opposite OAM terms. After filtering, this results in polarization-tunable configurations of bright spots moving across a desired intensity profile, with their number and direction fully customizable by design. This dual-functional approach leverages polarization as an additional degree of freedom, providing a compact, efficient, and fast solution for generating and controlling custom intensity patterns in 3D. The method can suggest a novel solution to dynamic light reshaping using integrated and versatile architectures, with promising applications for optical micromanipulation, tweezing, and trapping, in optofluidics [28] and quantum computing [29].

Funding. Project STRADA (Italian Presidency of the Council of Ministers); European Commission (PE0000001–program "RESTART").

Acknowledgment. This work was partially supported by the European Union under the Italian National Recovery and Resilience Plan (NRRP) of NextGenerationEU, partnership on "Telecommunications of the Future" (PE0000001–program "RESTART").

Disclosures. The authors declare no conflicts of interest.

Data availability. Data underlying the results presented in this paper are not publicly available at this time but may be obtained from the authors upon reasonable request.

Supplemental document. See Supplement 1 for supporting content.

REFERENCES

1. M. P. MacDonald, L. Paterson, K. Volke-Sepulveda, *et al.*, Science **296**, 1101 (2002).
2. D. G. A. Grier, Nature **424**, 810 (2003).
3. A. Forbes, M. de Oliveria, and M. R. Dennis, Nat. Photonics **15**, 253 (2021).
4. M. Mirhosseini, O. S. Magana-Loaiza, M. N. O'Sullivan, *et al.*, New J. Phys. **17**, 033033 (2015).
5. J. Wang, Sci. China Phys. Mech. Astron. **62**, 34201 (2019).
6. A. Holleczek, A. Aiello, C. Gabriel, *et al.*, Opt. Express **19**, 9714 (2011).
7. M. Liu, Y. Lei, L. Yu, *et al.*, Nanophotonics **11**, 3395 (2022).
8. Q. Zhan and J. R. Leger, Opt. Express **10**, 324 (2002).
9. T. Grosjean, D. Courjon, and C. Bainier, Opt. Lett. **32**, 976 (2007).
10. A. Sit, F. Bouchard, R. Fickler, *et al.*, Optica **4**, 1006 (2017).
11. M. De Oliveira, I. Nape, J. Pinnell, *et al.*, Phys. Rev. A **101**, 042303 (2020).
12. C. Rosales-Guzman, B. Ndagano, and A. Forbes, J. Opt. **20**, 123001 (2018).
13. C. A. Alonzo, P. J. Rodrigo, and J. Glückstad, Opt. Express **13**, 1749 (2005).
14. N. Hermosa, C. Rosales-Guzmán, and J. P. Torres, Opt. Lett. **38**, 383 (2013).
15. E. Engay, A. Bañas, A. I. Bunea, *et al.*, Opt. Commun. **433**, 247 (2019).
16. E. Medina-Segura, L. Miranda-Culin, V. Rodríguez-Fajardo, *et al.*, Opt. Lett. **48**, 4897 (2023).
17. A. V. Ustinov, S. N. Khonina, P. A. Khorin, *et al.*, J. Opt. Soc. Am. B **38**, 420 (2021).
18. S. N. Khonina, A. V. Ustinov, V. I. Logachev, *et al.*, Phys. Rev. A **101**, 043829 (2020).
19. S. N. Khonina, A. V. Ustinov, and A. P. Porfirev, Opt. Lett. **47**, 3988 (2022).
20. N. P. Hermosa, II and C. O. Manaois, Opt. Commun. **271**, 178 (2007).
21. Y. Zhang, X. Yang, and J. Gao, Sci. Rep. **8**, 4884 (2018).
22. F. Capasso, Nanophotonics **7**, 953 (2018).
23. A. Arbabi and A. Faraon, Nat. Photonics **17**, 16 (2023).
24. A. Vogliardi, G. Ruffato, D. Bonaldo, *et al.*, Sci. Rep. **13**, 10327 (2023).
25. A. Vogliardi, G. Ruffato, D. Bonaldo, *et al.*, Opt. Lett. **48**, 4925 (2023).
26. A. Vogliardi, G. Ruffato, D. Bonaldo, *et al.*, Nanophotonics **12**, 4215 (2023).
27. G. Ruffato, S. Brunetta, and H. Kobayashi, Opt. Commun. **517**, 128325 (2022).
28. Y. Yang, Y.-X. Ren, M. Chen, *et al.*, Adv. Photonics **3**, 034001 (2021).
29. X. Huang, W. Yuan, A. Holman, *et al.*, Prog. Quantum Electron. **89**, 100470 (2023).